Temporal local clustering coefficient uncovers the hidden pattern in temporal networks

Bofan Chen,[1,2] Guyu Hou,[1,3] and Aming Li[1,4,*]

[1]*Center for Systems and Control, College of Engineering, Peking University, Beijing 100871, People's Republic of China*
[2]*School of Economics, Peking University, Beijing 100871, People's Republic of China*
[3]*Academy for Advanced Interdisciplinary Studies, Peking University, Beijing 100871, People's Republic of China*
[4]*Center for Multi-Agent Research, Institute for Artificial Intelligence, Peking University, Beijing 100871, People's Republic of China*

(Received 22 July 2023; revised 13 March 2024; accepted 7 May 2024; published 5 June 2024)

Identifying and extracting topological characteristics are essential for understanding associated structures and organizational principles of complex networks. For temporal networks where the network topology varies with time, beyond the classical patterns such as small-worldness and scale-freeness extracted from the perspective of traditional aggregated static networks, the temporality and simultaneity of time-varying interactions should also be included. Here we extend the traditional analysis on the local clustering coefficient C in static networks and study the dynamical local clustering coefficient of temporal networks. We demonstrate that the temporal local clustering coefficient TC conveys the hidden information of nodes' neighboring connectance when interactions occur at various rhythms. By systematically analyzing various empirical datasets, we find that TC uncovers different interaction patterns in different types of temporal networks. Specifically, we show that TC has a strong positive correlation with C in efficiency-related networks, whereas they are uncorrelated in social activity-related networks. Moreover, TC helps to exclude interference from accidental interactions and reflect the actual clustering properties of network nodes. Our results shed light on the importance of digging into dynamical characteristics to fundamentally understand the underlying temporal structures of real complex systems.

DOI: 10.1103/PhysRevE.109.064302

I. INTRODUCTION

The complex network plays an essential role in our understanding of various complex systems, where nodes indicate system components and edges define the interactions between them [1–3]. It has deepened our insight into various scenarios, including social interactions [4], transportation [5], microbial population structure [6], etc. Numerous intriguing dynamics have been scrutinized within this specialized framework, such as the evolution of cooperation [7], epidemic processes [8], and synchronization [9], which greatly enhance our understanding of natural phenomena.

Understanding and describing the underlying patterns and properties of networks in different scenarios is the first but important step for further investigation. Over the past two decades, scientists from diverse backgrounds have constructed various models and measures to characterize different networks. For static networks, scale-free [10] and small-world [11] attributes are reported by extracting certain specific features, providing us with statistical insights into our daily interactions. Apart from these models that capture global properties, scientists have also proposed many other measures to quantify local properties of the static networks, such as the rich club coefficient [12–14], local clustering coefficient [15], community structure [16], to name a few.

However, real-world networks often undergo dynamic changes over time [17], making it challenging to uncover the underlying dynamic patterns solely through traditional static models or measures [7,18,19]. Recently, in the context of temporal networks, researchers have also defined a certain number of temporal measures based on their time-varying properties including temporal centrality [20], correlation [21], and motifs [22,23], which facilitate our understanding of systems' evolutionary dynamics. Although some of these measures are directly extended from the existing measures of static networks, they give more insightful inspirations. For example, based on the rich club coefficient, Pedreschi *et al.* [24] proposed the temporal rich club coefficient. Their important findings reveal that although certain datasets exhibit the rich club phenomenon in static networks, the frequent interactions among large-degree nodes may not be simultaneous or stable in the corresponding temporal networks.

The local clustering coefficient is a classical measure for a node in static networks, which quantifies how close its neighbors are to being a clique (every two neighbors are connected by edges). However, in the case of temporal networks, we cannot accurately capture the temporal clustering properties of nodes only through the local clustering coefficient. In other words, we lack information regarding whether the clustering interactions of nodes occur simultaneously or frequently.

To address this limitation, we propose the temporal local clustering coefficient in this paper, which takes into account the interaction time of nodes, enabling the investigation of nodes' clustering properties in temporal networks. We also evaluate our proposed measure by using a total of eight human activity datasets. We find that the proposed temporal local clustering coefficient can serve as an efficient identifier to distinguish different core-driven patterns of temporal networks like efficiency-related networks and social activity-related networks. Additionally, we also notice that the temporal local clustering coefficient can sensitively identify

*Corresponding author: amingli@pku.edu.cn

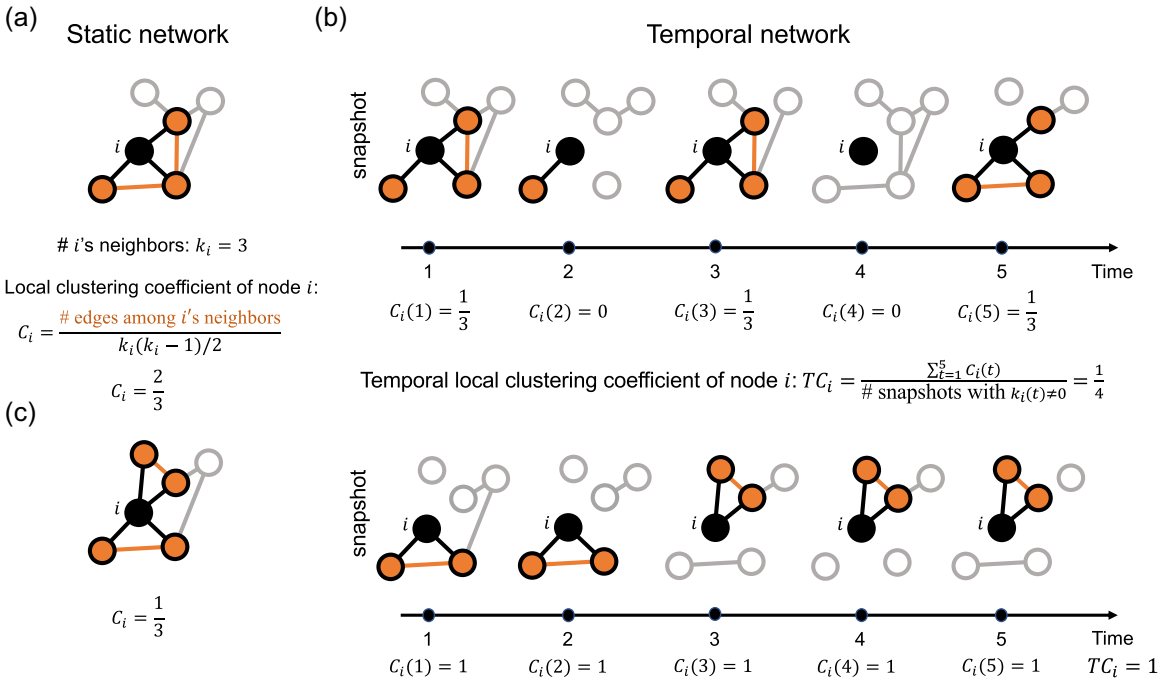

FIG. 1. Illustration of the concept of temporal local clustering coefficient. (a) A schematic illustration of a static network. The degree k_i of the black node i is three. The orange nodes are the neighbors of node i, and the local clustering coefficient (C_i) of node i is calculated through the orange edges among its neighbors divided by all the number of edges that could possibly exist among them. (b) A schematic illustration of a temporal network as a series of snapshots corresponding to the aggregated static network in panel (a). TC_i is computed by the average of $C_i(t)$ over each snapshot when $k_i(t) \neq 0$. (c) Example of the case where significant differences exist between TC_i and C_i for the temporal and corresponding static networks.

noise in temporal networks, enabling a more accurate reflection of the connections among nodes' neighbors. Finally, we discover different interaction patterns for various empirical datasets by comparing the underlying relationship between temporal and static local clustering coefficients.

II. THE TEMPORAL LOCAL CLUSTERING COEFFICIENT

There are many complex interactions in social activities that we can represent through networks. Rigorously, a temporal network $G = \{G_t | t \in \{1, 2, \ldots, T\}\}$ is composed of a series of snapshots $G_t = (\mathcal{V}, \mathcal{E}_t)$. Each snapshot is a network with a set of nodes $\mathcal{V} = \{1, 2, \ldots, N\}$ and a set of temporal edges $\mathcal{E}_t = \{e_1, e_2, \ldots, e_E | e_q = (i, j), i, j \in \mathcal{V}, q = 1, 2, \ldots, E\}$. In addition to the temporal network G, there exists a corresponding static network $G^s = (\mathcal{V}, \mathcal{L})$, where $\mathcal{L} = \bigcup_t \mathcal{E}_t$. In other words, the static network is obtained by aggregating all the snapshots over time [Figs. 1(a) and 1(b)]. Based on the static network, we can further define the weight of each edge $w_{ij} = |\Theta_{ij}|$, where $\Theta_{ij} = \{t | (i, j) \in \mathcal{E}_t\}$ is the set of occurrence times for each edge and $|\Theta_{ij}|$ indicates the number of elements in the set Θ_{ij}.

Our goal is to quantify the clustering phenomenon for every node in G while considering its temporality, that is, how close the neighbors are in each snapshot. We recall that for each node i in a static network, the local clustering coefficient C is defined by

$$C_i = \frac{|\{(j, k) | j, k \in \mathcal{V}_i, (j, k) \in \mathcal{L}\}|}{k_i(k_i - 1)/2}$$

(if $k_i \leqslant 1$, then $C_i = 0$), where $\mathcal{V}_i = \{j | (i, j) \in \mathcal{L}\}$ is the set of neighbors of node i and $k_i = |\mathcal{V}_i|$ is the degree of node i [Fig. 1(a)]. C_i is given by the number of edges among the nodes's neighbors divided by the number of edges that could possibly exist among them. C_i will be close to one if the neighbors of node i are closely connected, while C_i will be zero if none of its neighbors interact with each other.

To take into account the network temporality, we calculate the local clustering coefficients $C_i(t)$ and degrees $k_i(t)$ of node i over each snapshot G_t at time t. Then we combine information from all snapshots and define the temporal local clustering coefficient TC for node i as

$$TC_i = \frac{\sum_{t=1}^{T} C_i(t)}{\sum_{t=1}^{T} \mathbb{1}(k_i(t) > 0)}$$

(if $\sum_{t=1}^{T} \mathbb{1}(k_i(t) > 0) = 0$, then $TC_i = 0$), which is illustrated in Fig. 1(b). It can be interpreted as the average of $C_i(t)$ over the active period at which the degree of i satisfies $k_i(t) \geqslant 1$. Here, $\mathbb{1}(k_i(t) > 0)$ is an indicator function that equals one if $k_i(t) > 0$, and zero otherwise. From the definition, we can see that TC_i is computed from $C_i(t)$ of each snapshot. Figure 1(c) shows that even if the $C_i(t)$ of every snapshot is large, there is no guarantee that the static local clustering coefficient C_i should also be large. Since $C_i(t)$ and C_i are not directly related, the performance of TC_i and C_i can be distinct on different temporal networks. Only by satisfying the simultaneity of interactions, C_i can be similar to $C_i(t)$ and accordingly have a strong correlation with TC_i. Therefore, the value of TC_i not only depends on the closeness of the

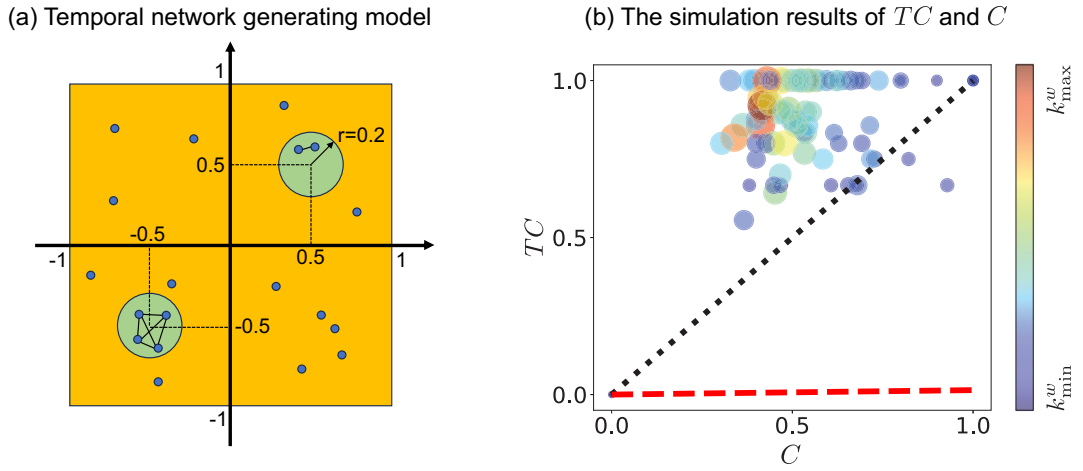

FIG. 2. Simulation results. (a) A schematic illustration of the temporal network generating model. There are $N = 100$ individuals wandering randomly in the finite plane of $[-1, 1] \times [-1, 1]$. Initially, the position of each individual is randomly distributed in the plane. At each time step, each individual moves a distance v in a random direction, where v follows a uniform distribution of [0,1]. If the movement hits the edge of the plane, it chooses another random direction and moves again. When nodes move together into the two green circular regions in the plane, they interact with each other. Repeating accordingly for $T = 100$ times, we obtain a simulated interaction temporal network with strong dynamic clustering property. (b) The difference between temporal local clustering coefficient TC and static local clustering coefficient C. The horizontal and vertical coordinates represent C and TC, respectively. For each node i, we calculate its C_i and TC_i, and then create a scatter plot to visualize the results. The degrees of nodes are shown in dots with different sizes: the larger the degree, the larger the size of the dot. The weighted degrees k^w (that is, the sum of the connected edges' weights) of nodes are shown in color. There are two reference lines in the figure: The black dotted line represents the reference line for $TC = C$; the red dashed line represents the reference line for $TC = pC$, where p is the average frequency of an edge interacting in a single snapshot, i.e., $p = (\frac{1}{T}\Sigma_1^T|\mathcal{E}_t|)/|\mathcal{L}|$ denotes the average of occurrences of all temporal edges divided by the number of edges in the static network. It is clear that TC is generally much larger than C in this strong clustering case, showing the superiority of TC.

interactions around the node i in the static network G^s, but also is closely related to the simultaneity of interactions around the node i.

To demonstrate the superiority of using the temporal local clustering coefficient to describe dynamic clustering properties, we calculate TC on synthetic data as in the proposed model in Ref. [9] and compare the difference between TC and C in this simulated scenario. As shown in Fig. 2(a), we assume that there are several individuals randomly walking in a plane. When some nodes move together into certain specific regions, they interact with each other together. Finally, the time-varying interactions between nodes will form a simulated temporal network. This model reflects the interaction network with strong dynamic clustering property in society, where individuals meet in the interaction region they all choose to interact with everyone around them. We find that the static local clustering coefficient C does not show a strong dynamic clustering property, which is only around 0.5. In contrast, the temporal local clustering coefficient TC of most nodes is close to one, which is much higher than C [Fig. 2(b)]. Therefore, in this strong clustering case, we present that TC is more suitable than C to capture the clustering properties of temporal networks.

III. *TC* OF EMPIRICAL TEMPORAL NETWORKS

To illustrate the significance of the temporal local clustering coefficient TC, we explore the dynamical patterns within temporal networks from eight empirical datasets. In these real datasets, the snapshots are constructed by aggregating social contacts over successive, nonoverlapping windows of Δt [Fig. 1(b)]. To ensure the robustness and reliability of our findings, we carefully select a time window that is relatively stable and appropriate for each dataset (see Appendix B). The time window we selected and the basic information of these datasets are presented in Table I. Specifically, US Air Traffic [24] represents the connections between US airports from January 2012 to September 2020. Hospital [25] represents the contacts between 29 patients and 46 healthcare workers in a hospital ward in France during five days. Ph.D. Exchange [26] describes math Ph.D. Exchange between universities based on a study of the Mathematics Genealogy Project. Workplace [27] represents the contacts between individuals measured in an

TABLE I. Information of empirical datasets. The table shows the names of the eight datasets studied in this paper, the time window of each snapshot, the number of snapshots (T), the total number of nodes (N), and the average degree of nodes ($\langle k \rangle$) in the static network.

Names of datasets	Time window	T	N	$\langle k \rangle$
US Air Traffic	10 month	10	1920	44.27
Hospital	300 min	16	75	30.37
Ph.D. Exchange	10 year	6	230	30.73
Workplace	1500 min	9	92	16.41
Primary School	50 min	20	242	68.73
High School	5 h	9	327	35.58
Village	20 h	16	86	8.07
SFHH Conference	15 min	86	403	47.47

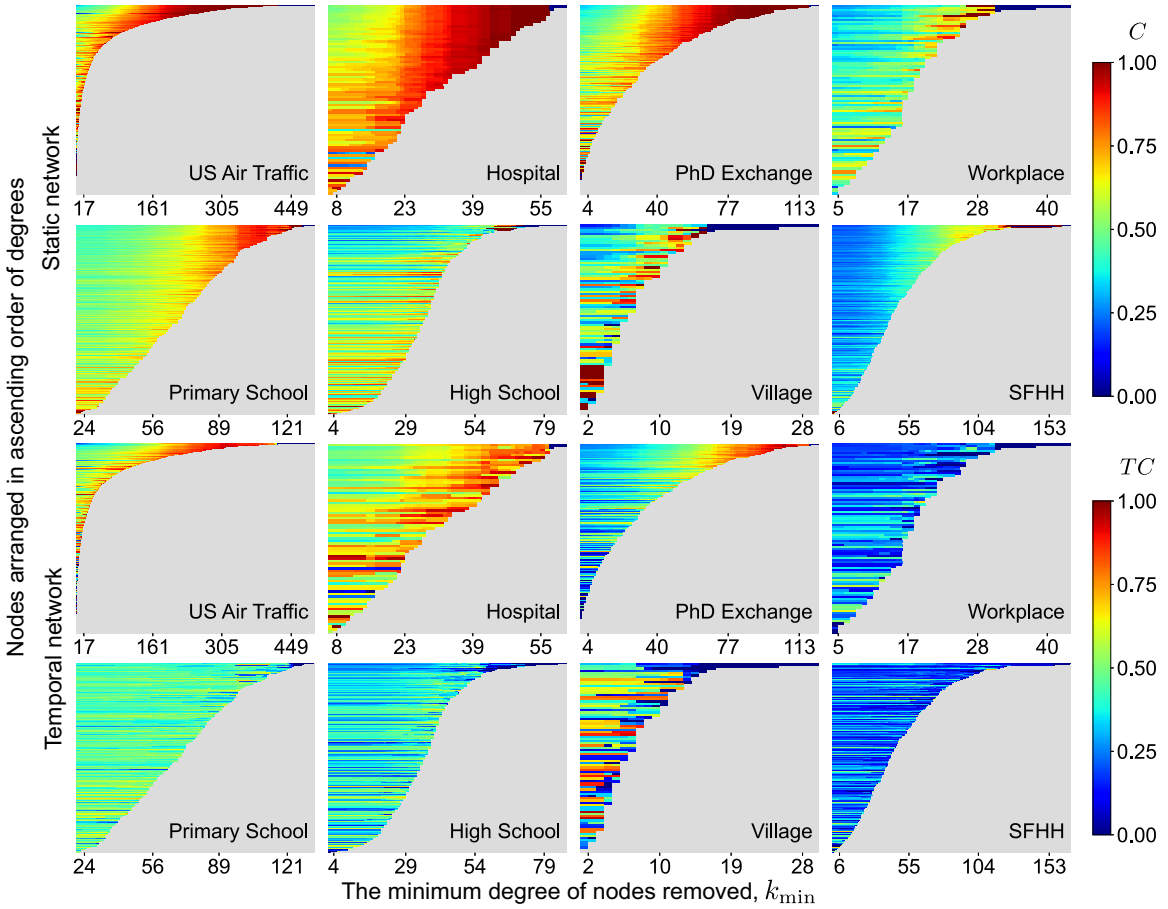

FIG. 3. Influence of $k_{\min}$ on C and TC. The first and last two rows of the figure show the influence of $k_{\min}$ on C and TC for each of the eight empirical datasets in Table I. The horizontal axis of the heatmaps represents the threshold values $k_{\min}$ of the static network below which the nodes are removed, and the vertical axis represents the nodes arranged in ascending order of their degrees. C and TC for each node are shown in color. The gray area in the figure means that the nodes under the threshold $k_{\min}$ have been removed from the network. Across all datasets, the majority of nodes exhibit an increase in C as $k_{\min}$ increases. For efficiency-related datasets, such as US Air Traffic, Hospital, Ph.D. Exchange, the value of TC increases with $k_{\min}$ for most nodes, mirroring the behavior of C. In contrast, for social activity-related datasets, such as Primary School, High School, Village, the value of TC decreases with $k_{\min}$ for most nodes, especially when $k_{\min}$ is set to a large value. At the same time, there are also datasets like Workplace and SFHH where TC shows little sensitivity to changes in $k_{\min}$. The varying behavior of TC as $k_{\min}$ shows that TC can be seen as an identifier to distinguish the core-driven patterns of temporal networks.

office building in France in 2015. Primary School [28,29] represents the contacts between students and teachers in a primary school. High School [30] represents contacts between students in a high school in France. Village [31] represents the contacts between 86 individuals living in a village in rural Malawi. SFHH Conference [27] represents the face-to-face interactions of 405 participants at the 2009 SFHH conference in France.

Due to the presence of noise in temporal networks derived from social data, we preprocess the data by setting a threshold value $k_{\min}$ for the minimum degree of nodes and $w_{\min}$ for the minimum weight of edges. This preprocessing step involves removing nodes with a degree lower than $k_{\min}$ and edges with a weight lower than $w_{\min}$, which are calculated from the aggregated static network. Choosing appropriate values for $k_{\min}$ and $w_{\min}$ is crucial because it helps to filter out accidental interactions (infrequent or incorrectly recorded interactions) that may interfere with our analysis. If the values are set too small, these accidental interactions might affect our results. Conversely, if the values are set too large, we risk losing significant information. Therefore, we investigate the effects of $k_{\min}$ and $w_{\min}$ on both the local clustering coefficient C and the temporal local clustering coefficient TC and observe interesting phenomena across different datasets.

Figure 3 illustrates the impact of $k_{\min}$ on both the local clustering coefficient C and the temporal local clustering coefficient TC. Initially, as $k_{\min}$ gradually increases from zero, the value of C of each node in the dataset remains relatively constant. Therefore, we select specific values of $k_{\min}$ for different datasets to exclude nodes with small degrees and filter out noise. As $k_{\min}$ continues to increase and approximately 50% of the nodes are removed, C of almost every node starts to rise. This phenomenon is known as the "rich club effect", where large-degree nodes tend to form tightly interconnected clusters. However, the behavior of TC is different from C. As $k_{\min}$ increases, efficiency-related temporal networks such as US Air Traffic, Hospital, and Ph.D. Exchange exhibit a trend towards stronger clustering among their high-degree nodes, reflected in TC approaching one [Fig. 3]. On the other

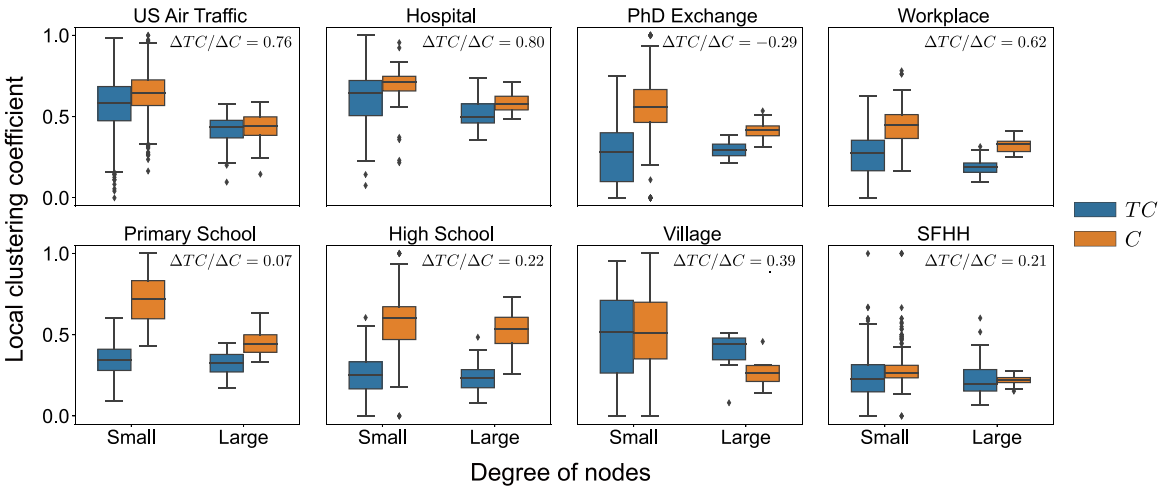

FIG. 4. The average temporal local clustering coefficient TC and static local clustering coefficient C of nodes with different degrees (k). The eight plots display the average TC and C values of nodes categorized by their degree (k) in different datasets. The horizontal axis separates the nodes into two groups based on whether their degree reaches half the degree of the largest node in the network, while the vertical axis represents the distribution of TC and C values of the classified nodes. TC is depicted in blue, while C is represented in yellow. The change of average TC and C from small-degree nodes to large-degree nodes are compared by the value $\Delta TC/\Delta C$, which is shown on the top right of each plot. Across most datasets, there is a negative correlation between C and k, indicating that nodes with higher degrees tend to have lower values of C. However, $|\Delta TC/\Delta C| < 1$ for all datasets, which means the correlation between TC and k is weaker, suggesting that TC is less influenced by the degree of nodes.

hand, social activity-related temporal networks like Primary School, High School, and Village show relatively low values of TC, indicating looser connections among their large-degree nodes. This difference suggests that in efficiency-related networks, the interactions between large-degree nodes maintain simultaneity, possibly due to the fixed working hierarchy within the network. For instance, in the air traffic dataset, there are more flights occurring simultaneously between airports with higher working hierarchies (e.g., major airports) to enhance work efficiency and maximize profits. In contrast, social activity-related networks exhibit more random interactions among their large-degree nodes, as these interactions do not necessarily depend on maintaining connectivity for the overall functioning of the system. Consequently, these interactions might not occur simultaneously. In this sense, TC plays a role of identifier. We can distinguish the core-driven pattern through the temporal clustering performance of nodes with large degrees, i.e., whether they still maintain rich club effects for temporal local clustering coefficients.

In addition, by comparing different nodes, we observe that the local clustering coefficient C tends to be higher for small-degree nodes compared with large-degree nodes [Fig. 4]. This phenomenon can be attributed to dilution, wherein the presence of excessive neighbors for large-degree nodes leads to a higher denominator when calculating C, resulting in lower C values. In fact, for large-degree nodes, the dilution effect is particularly pronounced when accidental interactions are present in the temporal network. In analyzing practical problems, the accidental interactions are noises, which should not be considered when we care about the clustering properties. However, these accidental interactions contribute additional neighbors to the large-degree nodes, significantly diluting their C values. However, in Fig. 4, TC does not present any significant correlation with degree k, which means that the temporal local clustering coefficient TC of large-degree nodes is not as easily diluted by accidental interactions compared with C.

This is because when calculating TC we average $C(t)$ over time, and those cases that are very fortuitous have a negligible effect on the results. The lower correlation between TC and k means that TC can effectively avoid noises from accidental interactions. This indicates that TC is more robust for capturing the connectivity among the neighbors of nodes, compared with C.

Figure 5 shows the influence of the $w_{\min}$ on C and TC. For datasets such as US Air Traffic, Village, Hospital, SFHH, and Ph.D. Exchange, increasing $w_{\min}$ leads to an increase in the C values of most nodes. This suggests that edges with larger weights in these datasets tend to form a triangular structure, resulting in a clustering of weights. In other words, edges with high weights tend to cluster among the neighbors of large-degree nodes. Conversely, in Primary School, High School, and Workplace, the C values of most nodes decrease as $w_{\min}$ increases. This implies that the distribution of weights on edges in these datasets is relatively random, and edges with high weights do not tend to form a triangular structure.

However, regardless of any specific datasets, the TC values decrease as $w_{\min}$ increases. This indicates that high-frequency interactions in the temporal networks are not simultaneous. In other words, even though nodes may have significant interactions with their neighbors, these interactions do not occur at the same time, suggesting a lack of synchronicity in the temporal patterns of interactions.

IV. THE *TC*-*C* PATTERNS

Having defined the temporal local clustering coefficient TC based on the local clustering coefficient C and explored

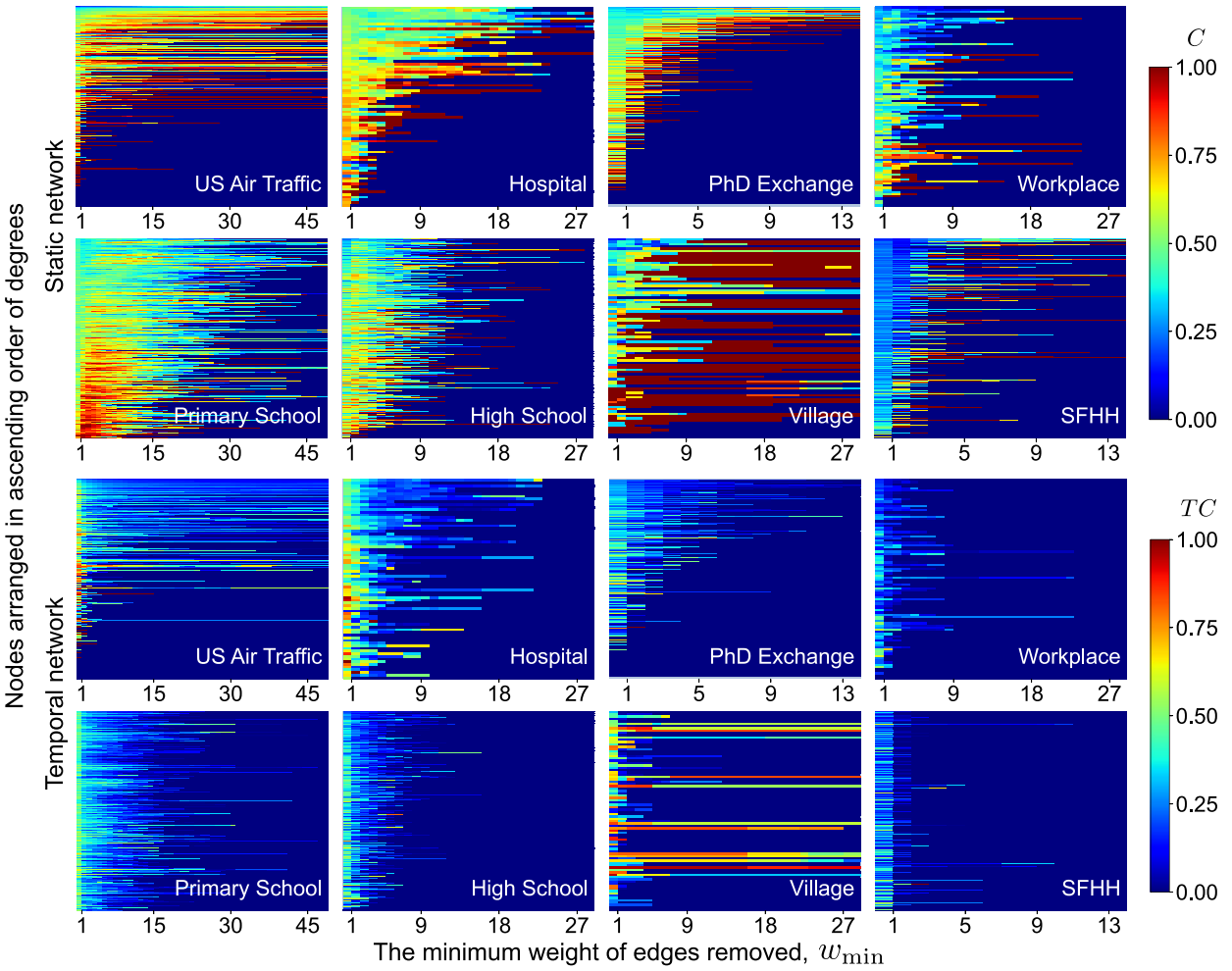

FIG. 5. Influence of $w_{\min}$ on C and TC. The first and last two rows of the figure show the influence of $w_{\min}$ on C and TC for each of the eight empirical datasets in Table I. The horizontal axis of the heatmaps represents the threshold values $w_{\min}$ of the static network below which the edges are removed, and the vertical axis represents the nodes in ascending order of their degrees. C and TC for each node are shown in color. In US Air Traffic, Village, Hospital, SFHH, and Ph.D. Exchange, the C of most nodes increases with $w_{\min}$; while in Primary School, High School, and Workplace, the C of most nodes decreases as $w_{\min}$ increases. In contrast, the TC of almost all datasets decreases as $w_{\min}$ increases. Since TC decreases dramatically with $w_{\min}$, in further discussions, $w_{\min} = 1$ is chosen for most datasets, except for Primary School and High School. For these two student datasets, $w_{\min} = 2$ is selected to exclude accidental interactions, as the C of the small-degree nodes in these datasets initially shows an upward jump with $w_{\min}$, indicating a higher rate of accidental interactions.

their properties under the influence of parameters $k_{\min}$ and $w_{\min}$, we find that the correlation between TC and C in different scenarios is different due to the different temporal properties of the temporal network. With this in mind, we hope to identify different interaction patterns through analysis of the correlation between TC and C, namely, TC-C patterns.

Figure 6 shows the TC-C scatter plots for different datasets from which we can detect five classes of temporal network TC-C patterns as follows.

Efficiency pattern. In datasets such as US Air Traffic and Hospital, the data points form a roughly straight line with a slope of one ($TC \approx C$). These networks prioritize maximizing working efficiency, leading to more interactions among nodes with higher work hierarchies. The clustering of weights phenomenon is observed in these networks, and there are fewer accidental interactions. The stability of interactions and the clustering of weights contribute to TC being close to C compared with the random temporal network where the data points are distributed around the red dash line ($TC \approx pC$, see Appendix A).

School pattern. In datasets like Primary School and High School, the data points are distributed approximately along a horizontal line. The C of students with more friends may be diluted by accidental contacts, while the TC remains unaffected and similar for all students. This pattern suggests that each student spends a similar proportion of time engaged in group activities, where interactions occur between every two members in the group.

Conference pattern. In the SFHH Conference dataset, the data points are distributed approximately along a vertical line. The C values of participants are similar, indicating similar interaction structures. However, the TC values exhibit wide distribution, with larger nodes tending to form interactions within group activities (resulting in higher TC for nodes with large degrees) and smaller nodes tending to form interactions in pairs (resulting in lower TC for nodes with small degrees).

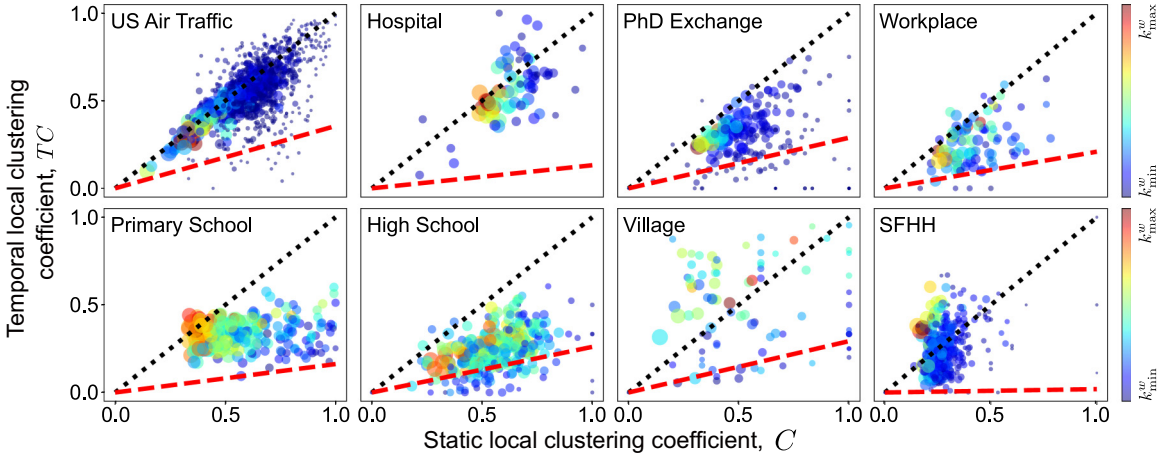

FIG. 6. The relation between temporal local clustering coefficient and local clustering coefficient. The eight scatter plots show the correlation of TC and C in different datasets. The horizontal and vertical coordinates represent C and TC, respectively. The size of a dot grows as its degree increases. The weighted degrees k^w (that is, the sum of the connected edges' weights) of nodes are shown in color. The black dotted line represents the reference line for $TC = C$; the red dashed line represents the reference line for $TC = pC$, where p is the average frequency of an edge interacting in a single snapshot, i.e., $p = (\frac{1}{T}\Sigma_1^T|\mathcal{E}_t|)/|\mathcal{L}|$ denotes the average of occurrences of all temporal edges divided by the number of edges in static network. From the figure, we can detect five classes of interaction patterns based on the distribution of data points.

Village pattern. In the Village dataset, the data points are more dispersed. TC values are generally larger than C for a significant number of nodes, indicating a preference for participating in group activities within the village.

Pair interaction pattern. In the Ph.D. Exchange and Workplace datasets, TC values are lower than C for almost all nodes. This suggests that nodes in these networks tend to engage in pair interactions rather than simultaneous interactions in groups.

V. DISCUSSION

In this paper, we propose the temporal local clustering coefficient for temporal networks to investigate the closeness and simultaneity of connections between neighbors of nodes. The TC can be regarded as an extension of the static network local clustering coefficient C, which not only shows the existence of interactions but also considers simultaneity and stability. According to the test on empirical datasets, TC gives more independent information compared with the concept of degree k and C. By comparing TC and C, we further identify the interaction patterns of different networks. Therefore, TC provides an extra value for the analysis of temporal networks in avoiding noises and identifying temporal patterns. In conclusion, our research reveals more information about the evolution of temporal networks, which helps better understand the underlying properties of dynamical complex systems.

Regarding future research, although there could be different definitions to describe the temporal clustering phenomenon [32], it would be more important to use theoretical analysis to prove the robustness of each conclusion. Besides, it would also be beneficial to consider other measures like TC and temporal rich club coefficient that capture the simultaneity and stability of edge interactions. For example, the TC only considers the properties of the first-order neighbors of the network nodes (i.e., triangular structure). We may further study patterns of high-order neighbors or other complex motifs [22,33]. Moreover, we can also explore the change of the static measures over time for temporal networks, such as whether $C_i(t)$ shows a certain pattern with t, etc.

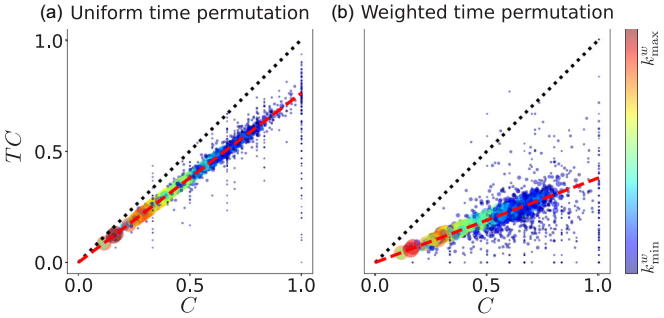

FIG. 7. The relation between temporal local clustering coefficient and local clustering coefficient after randomizing the original network. (a) Randomization of the US Air Traffic with the uniform time permutation method, where we keep the corresponding unweighted static network structure of the temporal network and randomly rearrange the interaction time of each edge. In this method, each edge will interact randomly with the same probability p at each moment. (b) Randomization of the US Air Traffic with the weighted time permutation method, where we keep the static network structure as well as the original weights distribution of the dataset. The weights of each edge are drawn from the given distribution, and the times of each interaction are uniformly distributed on the whole timeline based on the different weights of edges. The black dotted line represents the reference line for $TC = C$; the red dashed line represents the reference line for $TC = pC$, where p is the average frequency of an edge interacting in a single snapshot, i.e., $p = (\frac{1}{T}\Sigma_1^T|\mathcal{E}_t|)/|\mathcal{L}|$ denotes the average of occurrences of all temporal edges divided by the number of edges in static network. We can see that TC has a strong linear correlation with C under these two randomization methods.

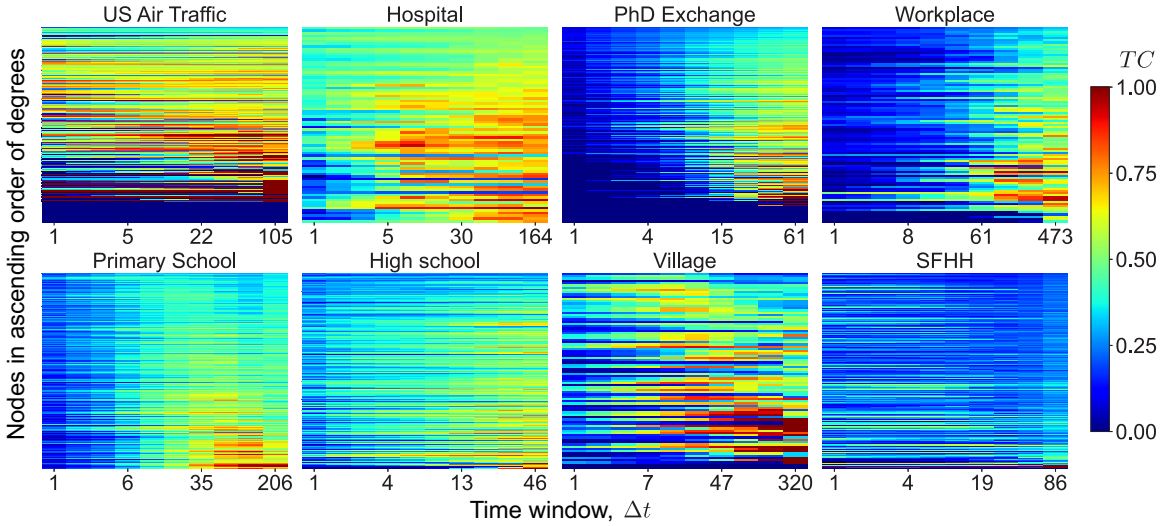

FIG. 8. Influence of time window Δt on the temporal local clustering coefficient. The eight heatmaps show the influence of time window Δt on temporal local clustering coefficient for eight empirical datasets. The horizontal coordinates represent the values of Δt, and the vertical coordinates represent each node in the order of smallest to largest degree. Given $k_{\min} = 1$, $w_{\min} = 1$ (for Primary School and High School $w_{\min} = 2$), TC for each node is shown in color. It is noticeable that TC is relatively stable when Δt takes a value in a suitable interval.

ACKNOWLEDGMENT

The authors would like to thank the anonymous referees for their constructive comments, and Wenqi Cao, Yao Meng for proofreading the manuscript.

APPENDIX A: METHODS FOR NETWORK RANDOMIZATION

To investigate the correlation between TC and C, we employ two randomization methods for the network analysis.

The first method is uniform time permutation [Fig. 7(a)], where we preserve the corresponding unweighted static network structure and randomly rearrange the appearance time of each edge. Each edge is randomly assigned a time of appearance with the same probability p at each moment. It can be inferred that TC is directly proportional to C, specifically $TC = pC$. In the US Air Traffic dataset, Fig. 7(a) demonstrates a strong correlation between TC and C, supporting our inference.

The second method is weighted time permutation [Fig. 7(b)]. Here, we randomize the temporal network while maintaining the original static network structure and weight distribution of the dataset. The weights of each edge are drawn from the given weight distribution, and the interaction times are uniformly distributed throughout the timeline based on the different edge weights. In Fig. 7(b), we observe that TC and C still exhibit a strong correlation in the US Air Traffic dataset, although the slope decreases compared with Fig. 7(a), indicating a disruption in the clustering of weights.

APPENDIX B: THE CHOICE OF TIME WINDOW Δt

The choice of the time window Δt is based on the concept of stability, ensuring that the temporal local clustering coefficient TC remains relatively stable within the selected Δt. In Fig. 8, we analyze the influence of Δt on TC while keeping $k_{\min} = 1$ and $w_{\min} = 1$ ($w_{\min} = 2$ for Primary School and High School) fixed for all datasets.

The results show that nodes with a small degree are more sensitive to changes in Δt compared with nodes with larger degrees. Additionally, TC generally tends to increase as Δt increases. We can roughly divide the change in TC into three stages. Initially, when Δt is very small, TC for all nodes is zero because there are no strictly simultaneous interactions according to our assumption that all interactions are transient. As Δt increases, TC grows and reaches a stable value that is less sensitive to further changes in Δt. Finally, as Δt approaches infinity, TC converges to the static network local clustering coefficient C.

Based on these observations, we select a Δt where TC becomes relatively insensitive to changes in the time window. This ensures that the chosen Δt captures the stable characteristics of the network's temporal dynamics while avoiding excessive sensitivity to small variations in Δt.

[1] R. Albert and A. Barabasi, Statistical mechanics of complex networks, Rev. Mod. Phys. **74**, 47 (2002).

[2] S. Dorogovtsev and J. Mendes, Evolution of networks, Adv. Phys. **51**, 1079 (2002).

[3] G. Flake, S. Lawrence, C. Giles, and F. Coetzee, Self-organization and identification of web communities, Computer **35**, 66 (2002).

[4] J. Boissevain and J. C. Mitchell, *Network Analysis: Studies in Human Interaction* (Walter de Gruyter GmbH & Co KG, Berlin, 2018).

[5] M. G. H. Bell and Y. Lida, *Transportation Network Analysis* (Wiley Online Library, Chichester, UK, 1997).

[6] M. S. Matchado, M. Lauber, S. Reitmeier, T. Kacprowski, J. Baumbach, D. Haller, and M. List, Network analysis methods

for studying microbial communities: A mini review, Comput. Struct. Biotechnol. J. **19**, 2687 (2021).
[7] A. Li, L. Zhou, Q. Su, S. P. Cornelius, Y.-Y. Liu, L. Wang, and S. A. Levin, Evolution of cooperation on temporal networks, Nat. Commun. **11**, 2259 (2020).
[8] N. Masuda and P. Holme, *Introduction to Temporal Network Epidemiology* (Springer, Singapore, 2017).
[9] S. N. Chowdhury, S. Majhi, M. Ozer, D. Ghosh, and M. Perc, Synchronization to extreme events in moving agents, New J. Phys. **21**, 073048 (2019).
[10] A.-L. Barabási and R. Albert, Emergence of scaling in random networks, Science **286**, 509 (1999).
[11] D. J. Watts and S. H. Strogatz, Collective dynamics of 'small-world' networks, Nature (London) **393**, 440 (1998).
[12] V. Colizza, A. Flammini, M. Serrano, and A. Vespignani, Detecting rich-club ordering in complex networks, Nat. Phys. **2**, 110 (2006).
[13] T. Opsahl, V. Colizza, P. Panzarasa, and J. J. Ramasco, Prominence and control: The weighted rich-club effect, Phys. Rev. Lett. **101**, 168702 (2008).
[14] M. P. van den Heuvel and O. Sporns, Rich-club organization of the human connectome, J. Neurosci. **31**, 15775 (2011).
[15] T. Opsahl, Triadic closure in two-mode networks: Redefining the global and local clustering coefficients, Soc. Networks **35**, 159 (2013).
[16] M. Girvan and M. E. Newman, Community structure in social and biological networks, Proc. Natl. Acad. Sci. U.S.A. **99**, 7821 (2002).
[17] P. Holme and J. Saramäki, Temporal networks, Phys. Rep. **519**, 97 (2012).
[18] A. Li, S. P. Cornelius, Y.-Y. Liu, L. Wang, and A.-L. Barabási, The fundamental advantages of temporal networks, Science **358**, 1042 (2017).
[19] I. Scholtes, N. Wider, R. Pfitzner, A. Garas, C. J. Tessone, and F. Schweitzer, Causality-driven slow-down and speed-up of diffusion in non-Markovian temporal networks, Nat. Commun. **5**, 5024 (2014).
[20] H. Liao, M. S. Mariani, M. Medo, Y.-C. Zhang, and M.-Y. Zhou, Ranking in evolving complex networks, Phys. Rep. **689**, 1 (2017).
[21] K.-I. Goh and A.-L. Barabási, Burstiness and memory in complex systems, Europhys. Lett. **81**, 48002 (2008).
[22] L. Kovanen, M. Karsai, K. Kaski, J. Kertész, and J. Saramäki, Temporal motifs in time-dependent networks, J. Stat. Mech.: Theory Exp. (2011) P11005.
[23] L. Kovanen, K. Kaski, J. Kertész, and J. Saramäki, Temporal motifs reveal homophily, gender-specific patterns, and group talk in call sequences, Proc. Natl. Acad. Sci. USA **110**, 18070 (2013).
[24] N. Pedreschi, D. Battaglia, and A. Barrat, The temporal rich club phenomenon, Nat. Phys. **18**, 931 (2022).
[25] P. Vanhems, A. Barrat, C. Cattuto, J.-F. Pinton, N. Khanafer, C. Rgis, B.-a. Kim, B. Comte, and N. Voirin, Estimating potential infection transmission routes in hospital wards using wearable proximity sensors, PLoS One **8**, e73970 (2013).
[26] D. Taylor, S. A. Myers, A. Clauset, M. A. Porter, and P. J. Mucha, Eigenvector-based centrality measures for temporal networks, Multiscale Model. Simul. **15**, 537 (2017).
[27] M. Génois and A. Barrat, Can co-location be used as a proxy for face-to-face contacts? EPJ Data Sci. **7**, 11 (2018).
[28] V. Gemmetto, A. Barrat, and C. Cattuto, Mitigation of infectious disease at school: targeted class closure vs school closure, BMC Infect. Dis. **14**, 695 (2014).
[29] J. Stehlé, N. Voirin, A. Barrat, C. Cattuto, L. Isella, J.-F. Pinton, M. Quaggiotto, W. Van den Broeck, C. Régis, B. Lina, and P. Vanhems, High-resolution measurements of face-to-face contact patterns in a primary school, PLoS One **6**, e23176 (2011).
[30] R. Mastrandrea, J. Fournet, and A. Barrat, Contact patterns in a high school: A comparison between data collected using wearable sensors, contact diaries and friendship surveys, PLoS One **10**, e0136497 (2015).
[31] L. Ozella, D. Paolotti, G. Lichand, J. P. Rodríguez, S. Haenni, J. Phuka, O. B. Leal-Neto, and C. Cattuto, Using wearable proximity sensors to characterize social contact patterns in a village of rural Malawi, EPJ Data Sci. **10**, 46 (2021).
[32] M. Latapy, T. Viard, and C. Magnien, Stream graphs and link streams for the modeling of interactions over time, Soc. Netw. Anal. Min. **8**, 61 (2018).
[33] R. Milo, S. Shen-Orr, S. Itzkovitz, N. Kashtan, D. Chklovskii, and U. Alon, Network motifs: Simple building blocks of complex networks, Science **298**, 824 (2002).